GLOBAL DISTRIBUTION OF ULTRAMAFIC LOW Ca PYROXENE ON THE MOON

Satoru Yamamoto[1], Ryosuke Nakamura[2], Tsuneo Matsunaga[1],Yoshiaki Ishihara[3], Takahiro Hiroi[4], Makiko Ohtake[3], Tomokatsu Morota[5], Naru Hirata[6], and Junichi Haruyama[3], [1]National Institute for Environmental Studies, Japan (yamachan@gfd-dennou.org), [2]National Institute of Advanced Industrial Science and Technology, Japan, [3]Japan Aerospace Exploration Agency, [4]Brown University, USA, [5]Nagoya University, Japan, and [6]The University of Aizu, Japan

INTRODUCTION

Recent observations of hyperspectral remote sensing for the Moon have revealed the existence of large exposed areas (LEAs) that are spectrally dominated by a lunar major mineral endmember: e.g., the purest anorthosite (PAN)[1,2], olivine-rich materials (ORM)[3], or low/high Ca-pyroxene (LCP/HCP) rich materials [4,5,6]. Each LEA typically spans several km wide sites, and is located at fresh craters or sloped areas on the crater walls or peaks.

This study focuses on LEAs of an ultramafic LCP (ULCP), which could originate from the early crystallization of the lunar magma ocean (LMO). While several previous studies have reported LCP-rich areas at local regions on the lunar surface, the occurrence trends of the ULCP are still unknown. For example, although it has been reported that the typical regoliths (mixing layer) in the highlands are spectrally dominated by LCP, these are mixtures of various minerals, not LEAs of ULCP. Thus, we conduct global surveys to find the global distribution of ULCP based on the hyperspectral data obtained by Spectral Profiler (SP) onboard Kaguya/SELENE [7].

METHOD

According to [8-10], a LCP with Ca amount $<\sim 10$ wt% and Mg# $>\sim$ 70-80 shows an 1 μm absorption band at wavelength λ shorter than $\sim$ 0.93 μm and a 2 μm absorption at shorter than $\sim$ 2 μm. In the global survey to find ULCP, we pick up spectra which show an 1 μm absorption band at $\lambda \leq \lambda_{\rm lcp} = 0.925\,\mu$m and with a 2 μm absorption band at $\lambda < 2.0\,\mu$m. In addition, we reject spectra with absorption depth less than 10 % to exclude mixtures of LCP and plagioclase, i.e., noritic anorthosite [5]. We also eliminate spectra showing 1.3 μm absorption band to avoid spectra reflecting the contamination by LCP with lower Mg# or HCP. Applying these algorithms to all the SP data ($\sim$ 70 million spectra), we found 247 ULCP points. Fig. 1 shows a representative spectrum of ULCP found by this survey, showing an 1 μm absorption band at $\lambda < 0.93\,\mu$m without a 1.3 μm absorption band, which is different from those of ORM, PAN, HCP-rich sites, and that in the mixing layer.

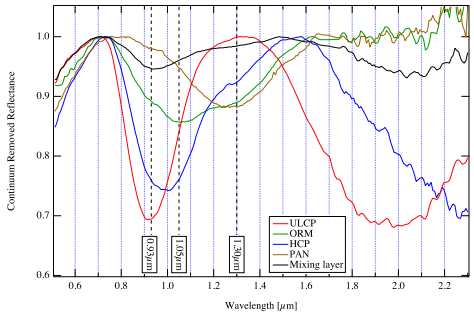

Figure 1: The continuum-removed reflectance spectra measured by SP at an ULCP-rich site at the Imbrium basin. For a comparison, the spectra for ORM, PAN, and HCP-rich sites, and a mixing layer by SP are plotted.

RESULTS

Fig. 2(a) shows the global distribution of the ULCP points found by this study. It is clear that the ULCP points are limited to the specific areas: the peak rings of the Imbrium basin, South-Pole Aitken (SPA) basin, and the rim of the Procellarum KREEP Terrane (PKT). In the Imbrium basin, most of the ULCP points are located around the Montes Alpes, where the ORM points are also detected [3]. We can also see many ULCP points in the SPA, in which they are found at conspicuous impact structures: e.g., Apollo, Antoniadi, Shrödinger, Lyman, and Zeeman basins/craters. In addition, there are several detection points at the edge of the PKT.

On the other hand, there is no ULCP in the Feldspathic Highland Terrane (FHT). Even when we include less ultramafic LCP for $\lambda_{\rm lcp} = 0.93\,\mu$m and 0.94 μm, we do not find the ULCP in the FHT, as shown in Figs. 2(b) and (c). Although the total number of the ULCP points increases with increasing $\lambda_{\rm lcp}$, the locations of the ULCP points are limited to the Imbrium, SPA, and PKT. Note that the Earth-based observations and the spectral analysis using SP data revealed that the mixing layers in the highlands are spectrally dominated by LCP [12-14]. However, typical spectra in the mixing layer show shal-

lower absorption bands and a discernible 1.3 μm, which are different from the characteristics of the ULCP. Thus, we can conclude that there is no ULCP point in the FHT.

One of the most intriguing features is that the Moscoviense and Crisium basins do not possess the ULCP points, while these two basins possess the ORM and PAN sites [2,3]. Note that these two basins have the thinnest crust on the Moon revealed by the GRAIL [15], suggesting that the formations of these impact basins could have excavated the upper mantle materials to expose on the lunar surface. Thus, the lack of the ULCP at these basins suggests that there is no ULCP-rich layer at depth less than the excavation depth of these basin formations below the PAN crust. In other words, our data and the GRAIL data suggest that the upper part of the lunar mantle is not dominated by the ULCP.

On the other hand, the ULCP points are distributed around the huge impact structures such as SPA and Imbrium. This suggests that the ULCP-rich layer exists at much deeper regions below the ORM layer. Fig. 3 illustrates the structures of the crust and mantle to explain the occurrence trends of the ULCP, ORM, and PAN. In this case, smaller basins such as the Moscoviense and Crisium could not excavate the ULCP layer, while the huge impacts that formed the SPA, Imbrium, and/or the putative Procellarum basins [5] could excavate the UCLP layer. The excavated ULCPs are distributed to the FHT regions, contributing to the LCP-dominant spectra of the mixing layer in the highlands. In summary, the occurrence trends of the ULCP are not consistent with a hypothesis that the upper part of the lunar mantle is dominated by ULCP. ULCP-rich layer exists at much deeper regions below the ORM-rich layer underlying the PAN crust.

Since the LMO scenario suggests that the ORM settled at the bottom of the mantle and then ULCP settled above the ORM layer, our model suggests that there is a reversed relation between ORM and ULCP. This may be explained by the mantle overturn or ORM-rich magmatic intrusions into the lower crust. However, in order to explain the lack of the KREEP exposures at the Crisium and Moscoviense basins [16,17], the mantle overturn scenario may be preferred.

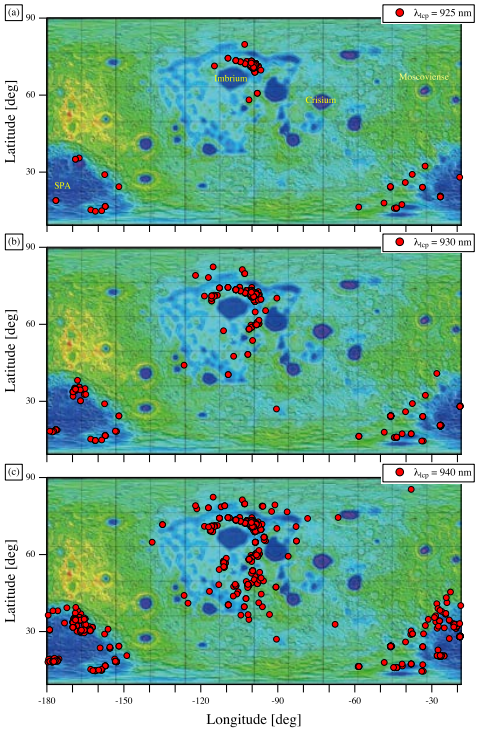

Figure 2: The global distributions of the ULCP-rich points with $\lambda_{\rm lcp}$ = (a) 925, (b) 930, and (c) 940 nm. The background is the total crustal thickness map [11].

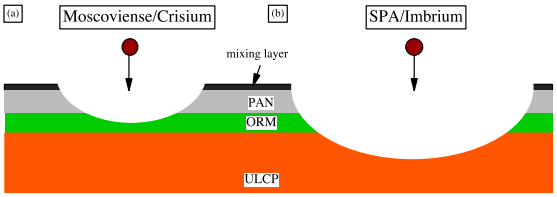

Figure 3: Schematic diagram of the excavations of the PAN, ORM, and ULCP materials to explain the occurrence trends of the LEAs for these minerals for (a) Moscoviense/Crisium and (b) the huge impact basins.

REFERENCES

[1] Ohtake, M. et al. (2009) Nature, 461, 236. [2] Yamamoto, S. et al. (2012) GRL, 39, L13201. [3] Yamamoto, S. et al. (2010) NGEO, 3, 533. [4] Nakamura, R. et al. (2009) GRL, 36, L22202. [5] Nakamura, R. et al. (2012) NGEO, 5, 775. [6] Yamamoto, S. et al. (2015) JGR, 120, 831. [7] Matsunaga, T. et al. (2008) GRL, 35, L23201. [8] Cloutis, E.A., & M.J. Gaffey (1991) JGR, 96, 22809. [9] Klima, R.L. et al. (2011), MAPS, 46, 379. [10] Denevi, B.W., et al. (2007) JGR, 112, E05009. [11] Ishihara, Y. et al. (2009) GRL, 36, L19202. [12] Hawke, B.R. et al. (2003) JGR, 108, 5050. [13] Lucey, P.G. (2014), Amer. Miner. 99, doi10.2138/am-2014-4854. [14] Melosh, H.J. et al. (2014) 45th LPSC, 2505. [15] Wieczorek, M.A. et al. (2013) Science, 339, 671. [16] Jolliff, B.L. et al. (2000) JGR, 105, 4197. [17] Yamashita, N. et al. (2010) GRL, 37, L10201.